Kink Instability in Applied-Field Magneto-Plasma-Dynamic Thrusters

M. Zuin,[1,2] R. Cavazzana,[1] E. Martines,[1] G. Serianni,[1] V. Antoni,[1,2] and M. Bagatin[1,2]
[1]*Consorzio RFX, Associazione EURATOM-ENEA sulla fusione, corso Stati Uniti 4, 35127 Padova, Italy*
[2]*Istituto Nazionale di Fisica della Materia, Unità di Padova, Italy*

M. Andrenucci, F. Paganucci, and P. Rossetti
Department of Aerospace Engineering, University of Pisa, Italy
and Centrospazio, Via A. Gherardesca 5, 56014 Pisa, Italy
(Received 14 November 2003; revised manuscript received 28 January 2004; published 3 June 2004)

Measurements of magnetic and electrostatic fluctuations in an applied field magneto-plasma-dynamic thruster have shown that a $m/n = 1/1$ kink mode becomes unstable whenever the Kruskal-Shafranov limit is violated. A positive correlation is established between the kink and performance degradation at high current, which has until now prevented the use of this kind of thruster in space missions.

DOI: 10.1103/PhysRevLett.92.225003 PACS numbers: 52.75.Di, 52.35.Py, 52.70.Ds

Magneto-plasma-dynamic (MPD) thrusters constitute a viable high power electric propulsion option for primary space missions, ranging from orbit raising to interplanetary transfer of large spacecrafts [1]. They operate as electromagnetic plasma accelerators, where acceleration is mainly provided by the Lorentz force produced by the interaction between the current and a self-induced magnetic field. A modified version of this kind of device is the applied field MPD thruster, which operates with an externally applied magnetic field, in addition to the self-generated one. The application of an external magnetic field has been shown to significantly improve the thruster performance at low current regimes [2]. However, the achievement of acceptable performance for space applications is hampered by the occurrence of detrimental phenomena, taking place when a critical current is exceeded [2]. This efficiency deterioration is due to the onset of critical regimes characterized by large fluctuations in the applied voltage signals and by damages to the anode [3]. These fluctuations have been interpreted in self-field MPDs in terms of plasma microinstabilities such as lower hybrid drift instability modified by finite-beta effects [4,5] or space charge instabilities [3] and in applied field devices such as shear Alfvén or compressional Alfvén waves [6,7], resulting from the conversion of $m = 0$ and $m = 1$ magnetohydrodynamic (MHD) modes. Whatever the origin, these instabilities have been indicated as the likely mechanism responsible for enhanced collisionality and anomalous resistivity, and therefore for enhanced input power. Thus, great effort is presently devoted to investigate the origin and the role of plasma instabilities on the onset of critical regimes.

In this Letter we report for the first time evidence of the onset of gross MHD instabilities in an applied field MPD thruster that have been identified as kink modes with azimuthal (m) and axial (n) periodicity $m/n = 1/1$. An instability threshold has been recognized and it has been found that the onset of these instabilities corresponds to the setting up of the critical regimes mentioned above. Such a finding opens up new scenarios for improving the efficiency of this kind of thrusters.

The MPD thruster object of our investigation is a device named hybrid plasma thruster (HPT) [2]. A schematic of the HPT is shown in Fig. 1, where a cylindrical system of coordinates is introduced ($z = 0$ is located at the thruster outlet). To reduce the electrode erosion, the thruster has a central hollow multichannel cathode, which consists of 19 copper tubes with a diameter of 8.5 mm, housed inside a holder tube 44 mm in diameter. The anode consists of eight straps, equally spaced in the azimuthal direction and each 20 mm wide. The straps are surrounded by an aluminum cylinder with a diameter of 150 mm, mounted coaxially to the thruster, electrically insulated from both electrodes, acting like a flux conserver for the plasma column. More details on the HPT and experimental setup are reported in Ref. [2].

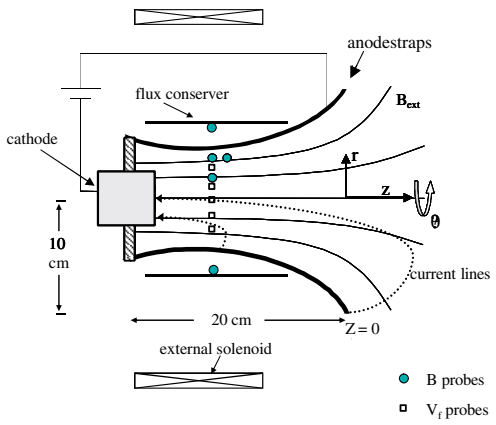

FIG. 1 (color online). Schematic of the HPT, showing external magnetic field lines, external solenoid, position of magnetic and electric probes, and two examples of current lines.

An external axial magnetic field B_{ext} up to 100 mT on the thruster axis can be applied by means of a solenoid. It is worth noting that in the HPT magnetic field lines do not link the cathode and the anode, as shown in Fig. 1. This feature makes the device topologically different from coaxial guns used for helicity injection in spheromaks [8]. The device is mounted on a thrust stand inside a cylindrical vacuum chamber (length 3.5 m, radius 0.6 m), electrically insulated from both anode and cathode, where a back pressure of the order of 10^{-2} Pa during the pulse is maintained. The chamber is large compared to the plasma dimensions, so that boundary effects can be assumed negligible in determining the discharge behavior. The thruster is powered by a pulse forming network, which allows quasisteady current pulses (I_{tot}) lasting 2.5 ms, as shown in Fig. 2. The magnetic field solenoid is powered by a dc generator, switched on a few seconds before the discharge. The propellant (argon in this case) is injected by a gas feeding system, which provides a constant gas refueling of 660 mg/s during the plateau phase. Experimental conditions with I_{tot} between 1.5 and 9 kA and B_{ext} between 5 and 100 mT have been explored. Typical plasma parameters are $n_e \approx 10^{20}$ m^{-3} and $T_e \approx$ 5–10 eV [2]. The Alfvén time is of a few μs, while the resistive diffusion time is of the order of 100 μs.

In order to investigate the spatiotemporal properties of the plasma fluctuations, three arrays of magnetic and electric probes have been used. The first system consists of six triaxial magnetic probes housed in quartz tubes, each tube containing two probes spaced by 15 mm. All quartz tubes have been inserted parallel to the main axis, two of them located at $r = 41$ mm, azimuthally spaced by $\pi/4$, the third at $r = 18$ mm. The most inserted probes have been located at $z = -109$ mm (see Fig. 1). Each magnetic probe measures the three field components by three nested coils. The second system consists of four external biaxial magnetic coils, mounted on the inner surface of the flux conserver, measuring axial and azimuthal magnetic fluctuations in four equally spaced azimuthal positions. The third system is a circular array of eight equally spaced Langmuir probes, measuring floating potential V_f, 31 mm radially spaced from the axis.

Figure 2 shows typical waveforms of the discharge current I_{tot}, the voltage difference between anode and cathode ΔV, the azimuthal magnetic field B_θ, measured by the insertable probe at $r = 41$ mm, and the axial magnetic field B_z, measured by the probe close to the axis (both at $z = -109$ mm). The latter two quantities have been obtained through numerical integration of the probe signals; however, since the probe sampling starts after B_{ext} is switched on, the B_z signal cannot include such a field, which is constant throughout the discharge.

The signals reveal that a large B_z of about 25 mT is generated by the current flowing in the plasma, so that the externally applied field ($B_{\text{ext}} = 100$ mT in this case) is significantly increased, i.e., the discharge has a paramagnetic behavior. Strong fluctuations are observed on all signals during the discharge. The temporal evolution of the four external B_z's and of the inner measurements for B_r, B_θ, and B_z close to the thruster axis is shown in Fig. 3 for an expanded time window during the stationary phase of the discharge. In the same figure the eight floating potential signals are also shown. A regular large oscillation at a frequency of the order of 100 kHz can be observed in all the signals, with the same azimuthal propagation and speed, for both magnetic and electrostatic signals, confirming that they are both signatures of the same process. These oscillations have an $m = 1$ azimuthal periodicity. The $m = 1$ mode is observed to grow a few microseconds after $t = 0$, and then to oscillate during the plateau phase. The phase of the mode changes linearly with time, as a result of the azimuthal rotation. The mode frequency is almost proportional to I_{tot} (ranging from 30 to 100 kHz for $1.5 < I_{\text{tot}} < 9$ kA, corresponding to a rotation velocity of about 20 km/s at $r =$ 41 mm), while it slightly depends on B_{ext}. The propagation direction changes sign when the external field is

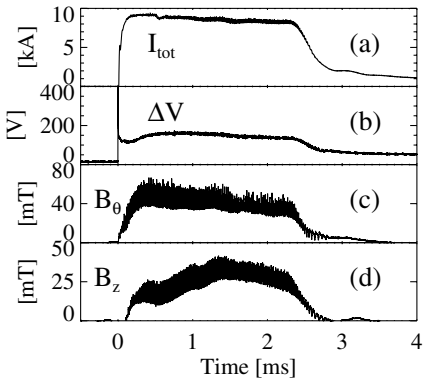

FIG. 2. Time history of a typical discharge: (a) total current I_{tot}, (b) potential difference ΔV, (c) B_θ measured at $r =$ 41 mm, (d) B_z measured at $r = 18$ mm.

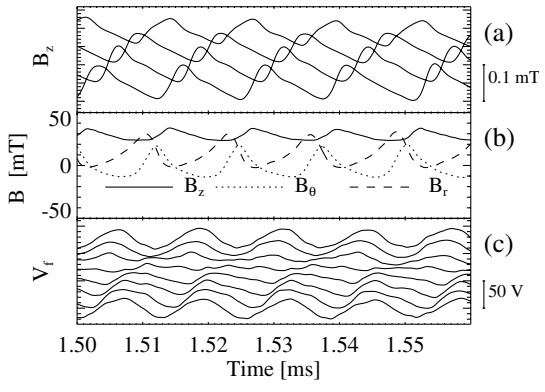

FIG. 3. Temporal evolution of (a) B_z signals close to the flux conserver (the scale refers to one signal, the others having been vertically shifted by 0.05 mT), (b) B_r, B_θ, B_z measured at $r =$ 18 mm, (c) V_f signals (vertically shifted by 18 V).

reversed and is consistent with the direction of an $\mathbf{E} \times \mathbf{B}$ drift. Frequency and amplitude measurements performed by means of the external probes have shown that the insertion of the internal diagnostic system does not significantly modify the plasma dynamics.

The axial structure of the mode has been analyzed by means of two axially spaced magnetic probes located at $r = 41$ mm. The spectral density $S(k_z, f)$, where k_z is the wave vector in the axial direction and f is the frequency, has been deduced by means of a two-point statistical technique [9]. Values of k_z ranging from 10 to 60 m^{-1} have been obtained, corresponding to wavelengths from 0.1 to 0.6 m. Measurements in different experimental conditions (I_{tot} and B_{ext}) have confirmed the almost linear increase of the frequency with the current (as already mentioned) and have shown that the axial wavelength increases with B_{ext}, as shown in Fig. 5. It must be noted that in other open systems the observation of only discrete wave vectors has been attributed to a local discontinuity on the Alfvén velocity acting as a virtual boundary for the system [10]. Optical measurements in high B_{ext} regimes [2] show that the plasma plume extends up to 0.4 m outside from the thruster outlet, so that the total plasma column length L is about 0.6 m, comparable to the axial wavelength measured in the same experimental conditions. As a consequence the mode results in winding once azimuthally for an equivalent $n = 1$ axial periodicity. We can thus conclude that it is an $m/n = 1/1$ helical kink mode.

At a given B_{ext}, a significant fluctuation level is observed only when I_{tot} is larger than a threshold value. Above this threshold, the amplitude grows with I_{tot}. An example of this behavior is shown in Fig. 4 for $B_{\mathrm{ext}} =$ 5 mT. In the same figure the V-I characteristic of the discharge is also shown. It is remarkable that the onset of the mode happens at the current level where a change in the slope of the characteristic is found. Such a change corresponds to the onset of the critical regime mentioned above where the efficiency of the thruster is degraded due to the rapidly increasing power required to sustain the discharge [2,3]. This suggests that the kink mode is responsible for the critical regime.

The basic geometry of the applied field MPD thruster, with its combination of almost parallel current and applied field, places it within a wide category of devices, which can generally be labeled as screw pinches [11]. A general feature of screw pinches is that, when some threshold of the ratio between current and applied magnetic field is exceeded, current driven large scale MHD instabilities are excited, with effects which range from changes in the topology of the discharge to its disruption [11]. Such MHD instabilities, which can lead to an amplification of the applied magnetic flux, linked to a spontaneous reorganization of the current density pattern inside the device [12,13], tend to develop whenever the condition $\mathbf{k} \cdot \mathbf{B} = 0$ is satisfied ($\mathbf{k}$ is the perturbation wave vector). This condition corresponds to perturbations having the same pitch as the unperturbed magnetic field lines. In a cylinder of length L and radius r the $\mathbf{k}$ components assume the discrete values $k_\theta = m/r$ and $k_z = 2\pi n/L$, with m and n integers. The condition can thus be written in terms of the safety factor $q(r) = rB_z/(L/2\pi)B_\theta$ as $q(r) = m/n$. In particular, the MHD stability criterion dubbed Kruskal-Shafranov criterion [12] prescribes that q must be greater than 1 in the plasma column in order to avoid the growth of an $m/n = 1/1$ kink instability. In the applied field MPD thruster the situation is more complex than in an ideal screw pinch, due to the presence of a radial current density, which allows the current to flow from the anode to the cathode. As a consequence, the axial current is not constant along the plasma column, but decreases with increasing z. For the present analysis, the axial current I_{exp} at the probe axial position has been directly obtained by measuring B_θ close to the anode and applying Ampere's law.

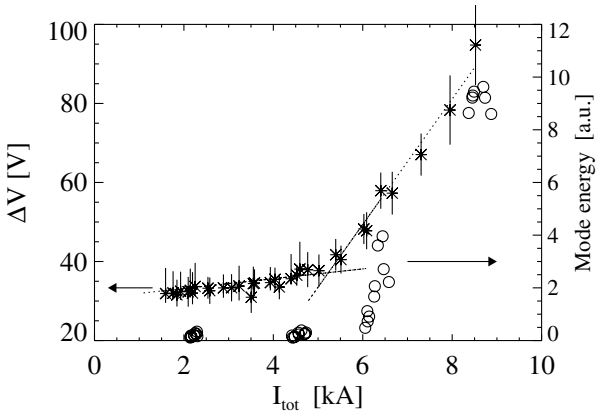

FIG. 4. Potential difference between anode and cathode (stars) and total mode energy (circles) plotted as a function of the discharge current I_{tot}, for $B_{\mathrm{ext}} = 5$ mT.

In Fig. 5 the ratio of the measured I_{exp} over the total current flowing to the cathode I_{tot} in different experimental conditions is plotted. It shows that at high B_{ext} the whole current is encompassed by the circumference in which the B_θ probe lies, therefore confirming that the plasma column extends beyond the corresponding axial position. At low B_{ext} only a fraction of the total plasma current is detected at $z = -109$ mm, with current lines mostly radially linking the cathode to the anode at $z < -109$ mm. Increasing B_{ext} has the effect of axially stretching the current channel, forcing a larger fraction of the current to close at the anode at $z > -109$ mm. The lower B_{ext}, the lower the ratio $I_{\mathrm{exp}}/I_{\mathrm{tot}}$. It is worth noting that the column length shows the same dependence on B_{ext} exhibited by the experimental wavelength in the axial direction, allowing to extend to different B_{ext} experimental conditions the validity of the previous assumption of the $n = 1$ mode periodicity. This hypothesis is further confirmed by recent experimental investigations of $m/n = 1/1$ helical instability by means of a

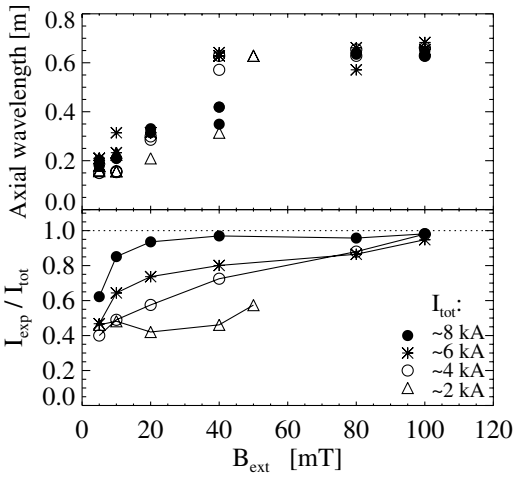

FIG. 5. Axial wavelength (top) and ratio between the measured I_{exp} and I_{tot} (bottom) plotted as a function of B_{ext}, for four different total current regimes.

fast CCD camera in a similar open system as coaxial gun device [10]. In this device, where, unlike the MPD, a direct flux link is always established between cathode and anode, the kink is shown to modify the direction of the current channel from axial to azimuthal, in a paramagnetic process that is demonstrated to amplify the applied B_{ext}.

In a paramagnetic system q is expected to be a decreasing function of the radius so that the Kruskal-Shafranov criterion prescribes $q > 1$ at the edge of the plasma column. This criterion can be written in terms of the parameter $\lambda = \mu_0 I/\Psi$, where I is the plasma current and Ψ is the flux of the externally applied axial magnetic field. The stability threshold for the $m/n = 1/1$ mode is thus given by $\lambda = 4\pi/L$, and the region of stability corresponds to $\lambda < 4\pi/L$. The experimental values of λ, computed for different experimental conditions and assuming a plasma column radius of 40 mm, are shown in Fig. 6 as a function of the plasma column length L. Stable and unstable cases have been sorted out according to a threshold on the mode energy, namely, 10% of the maximum mode energy observed over all the experimental conditions at a given B_{ext} value. The choice of the threshold does not affect the final result, due to the fast increase in mode energy observed beyond the stability threshold (see Fig. 4). The result shows an excellent agreement with the theoretical Kruskal-Shafranov limit, plotted as a dashed line. In the same figure the experimental conditions predicted to be critical according to an empirical model described in [2] are indicated with a cross. It is found that critical regimes coincide with cases showing the presence of a kink mode. Therefore the results prove that critical regimes are related to a large MHD kink instability, growing in the presence of a $q = 1$ resonant surface in the plasma.

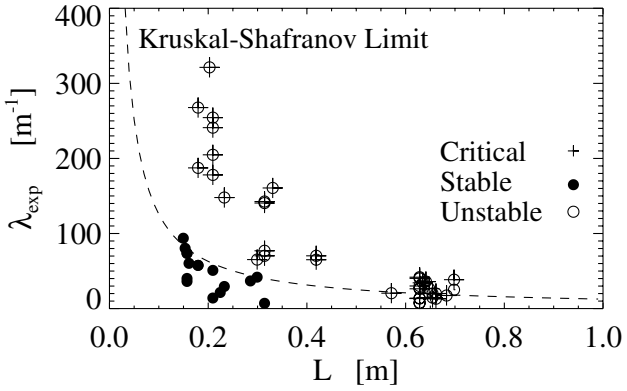

FIG. 6. λ_{exp} as a function of the plasma column length L. Dashed line is the Kruskal-Shafranov limit, dividing stable/unstable regions. Crosses mark critical regime conditions.

Though not addressed in this Letter, the increase in effective impedance and the efficiency reduction observed in critical regimes can be understood by drawing an analogy with some fusion relevant systems such as the reversed field pinch [12] and spheromak [14] configurations, where the development of kink modes is known to lead to an increase of the power required to sustain the discharge.

The authors wish to thank V. Cervaro, N. Pomaro, L. Ranzato, M. Recchia, and A. Saglia. This work has been granted by Italian Space Agency (ASI).

[1] R. G. Jahn, *Physics of Electric Propulsion* (McGraw-Hill, New York, 1968).
[2] M. Andrenucci *et al.*, in *Proceedings of the 28th International Electric Propulsion Conference, Toulouse, France, 2003* (CNES, Toulouse, 2003).
[3] H. P. Wagner, H. J. Kaeppeler, and M. Auweter-Kurtz, J. Phys. D **31**, 519 (1998).
[4] E. Y. Choueiri, Phys. Plasmas **6**, 2290 (1999).
[5] D. C. Black, R. M. Mayo, and R. W. Caress, Phys. Plasmas **4**, 3581 (1997).
[6] R. Hatakeyama, M. Inutake, and T. Akitsu, Phys. Rev. Lett. **47**, 183 (1981).
[7] Y. Amagishi *et al.*, J. Phys. Soc. Jpn. **71**, 2164 (2002).
[8] P. M. Bellan, *Spheromaks* (Imperial College, London, 2000).
[9] J. M. Beall, Y. C. Kim, and E. J. Powers, J. Appl. Phys. **53**, 3933 (1982).
[10] S. C. Hsu and P. M. Bellan, Phys. Rev. Lett. **90**, 215002 (2003).
[11] J. P. Freidberg, *Ideal Magneto-Hydro-Dynamics* (Plenum, New York, 1987).
[12] S. Ortolani and D. D. Schnack, *Magnetohydrodynamics of Plasma Relaxation* (World Scientific, Singapore, 1993).
[13] J. B. Taylor, Rev. Mod. Phys. **58**, 741 (1986).
[14] P. K. Browning *et al.*, Phys. Rev. Lett. **68**, 1718 (1992).